

See discussions, stats, and author profiles for this publication at: <https://www.researchgate.net/publication/14704517>

Stress and strain in staphylococcal nuclease

ARTICLE *in* PROTEIN SCIENCE · MAY 1993

Impact Factor: 2.85 · DOI: 10.1002/pro.5560020513 · Source: PubMed

CITATIONS

15

READS

24

4 AUTHORS, INCLUDING:



Roger Kautz

Northeastern University

25 PUBLICATIONS 1,010 CITATIONS

[SEE PROFILE](#)



Robert O. Fox

University of Houston

67 PUBLICATIONS 3,444 CITATIONS

[SEE PROFILE](#)

Stress and strain in staphylococcal nuclease



ALEC HODEL,^{1,2} ROGER A. KAUTZ,^{1,3} MARC D. JACOBS,¹ AND ROBERT O. FOX^{1,2}

¹ Department of Molecular Biophysics and Biochemistry and

² The Howard Hughes Medical Institute, Yale University, New Haven, Connecticut 06511

(RECEIVED August 3, 1992; REVISED MANUSCRIPT RECEIVED December 21, 1992)

Abstract

Protein molecules generally adopt a tertiary structure in which all backbone and side chain conformations are arranged in local energy minima; however, in several well-refined protein structures examples of locally strained geometries, such as *cis* peptide bonds, have been observed. Staphylococcal nuclease A contains a single *cis* peptide bond between residues Lys 116 and Pro 117 within a type VIa β -turn. Alternative native folded forms of nuclease A have been detected by NMR spectroscopy and attributed to a mixture of *cis* and *trans* isomers at the Lys 116-Pro 117 peptide bond. Analyses of nuclease variants K116G and K116A by NMR spectroscopy and X-ray crystallography are reported herein. The structure of K116A is indistinguishable from that of nuclease A, including a *cis* 116–117 peptide bond (92% populated in solution). The overall fold of K116G is also indistinguishable from nuclease A except in the region of the substitution (residues 112–117), which contains a predominantly *trans* Gly 116–Pro 117 peptide bond (80% populated in solution). Both Lys and Ala would be prohibited from adopting the backbone conformation of Gly 116 due to steric clashes between the β -carbon and the surrounding residues. One explanation for these results is that the position of the ends of the residue 112–117 loop only allow *trans* conformations where the local backbone interactions associated with the ϕ and ψ torsion angles are strained. When the 116–117 peptide bond is *cis*, less strained backbone conformations are available. Thus the relaxation of the backbone strain intrinsic to the *trans* conformation compensates for the energetically unfavorable *cis* X-Pro peptide bond. With the removal of the side chain from residue 116 (K116G), the backbone strain of the *trans* conformation is reduced to the point that the conformation associated with the *cis* peptide bond is no longer favorable.

Keywords: NMR; proline isomerism; staphylococcal nuclease; X-ray crystallography

Protein molecules generally adopt a tertiary structure in which backbone and side chain conformations are arranged in local energy minima. Strained conformations such as *cis* peptide bonds or eclipsed side chain rotamers are rarely found. However, in several well-refined protein structures, examples of such locally strained geometries have been observed, usually involving a residue in the enzyme active site (Herzberg & Moult, 1991). Clearly, in such cases, some kind of stress, or deforming force, inherent in the structure must cause the resulting strain, or deformation. While the quality of the crystal structures involved leaves little doubt concerning the correctness of these observations, the mechanism by which the stress is imposed in order to favor locally strained conformations remains unclear.

We have examined the relationship between stress and strain in staphylococcal nuclease A, the Ca^{2+} -dependent nuclease of *Staphylococcus aureus*, strain Foggi. Staphylococcal nuclease, a small protein (149 residues) lacking disulfide bridges, has been the subject of many early protein folding studies (reviewed in Tucker et al. [1979]) and of recently renewed interest (Calderon et al., 1985; Serspersu et al., 1986; Shortle & Meeker, 1986; Kuwajima et al., 1991). The crystal structures of nuclease (Kinemage 1; Hynes & Fox, 1991) and the nuclease- Ca^{2+} -pdTp complex (Cotton et al., 1979; Loll & Lattman, 1989) have been refined to high resolution. Nuclear magnetic resonance studies of nuclease revealed a slow exchange between two folded conformations that was proposed to be due to a mixture of *cis* and *trans* isomers at the Lys 116-Pro 117 peptide bond (Markley et al., 1970; Fox et al., 1986; Wang et al., 1990). This hypothesis was confirmed by an extensive NMR kinetic analysis (Evans et al., 1989) and examination of two proline mutants, Pro 117 → Gly (P117G) and Pro 117 → Thr (P117T) (Evans et al.,

Reprint requests to: Robert O. Fox, Department of Molecular Biophysics and Biochemistry, 260 Whitney Avenue, Yale University, New Haven, Connecticut 06511.

³ Present address: Department of Chemistry, Massachusetts Institute of Technology, Cambridge, Massachusetts 02139.

1987; Kautz & Fox, 1991), which display only single resonances for each histidine H^{e1} proton, in contrast to the pairs of resonances characteristic of nuclease A (Fox et al., 1986) (see Fig. 1A) and all mutants at positions other than Pro 117 (Alexandrescu et al., 1990).

Unfolded nuclease and a peptide analogue of this segment favor the *trans* isomer of the Lys 116-Pro 117 peptide bond (Evans et al., 1987; Raleigh et al., 1992). Thus,

the *cis* configuration found in the native molecule must be a strained element. We consider two possible explanations for why the folded protein favors the strained *cis* isomer. First, the *cis* conformation could be stabilized by energetically favorable tertiary interactions that do not exist in the *trans* form. The energy of such tertiary interactions would compensate for the added strain of the *cis* peptide bond. Alternatively, the ends of the β -turn peptide segment are restrained by the protein fold such that the local backbone interactions of all accessible conformations with a *trans* 116–117 peptide bond are more strained and energetically less favorable than those of the observed type VI_a β -turn conformation containing a *cis* peptide bond. To discriminate between these possibilities we have prepared two nuclease variants containing single amino acid substitutions within this type VI_a β -turn.

We focused our initial attention on Lys 116, which participates directly in the *cis* peptide bond with Pro 117. We reasoned that the Lys 116 side chain may limit the conformational space explored by the peptide segment or make unfavorable van der Waals contacts with the remainder of the β -turn in the *trans* configuration. A Gly 116 variant (K116G) and an Ala 116 variant (K116A) were prepared by site-directed mutagenesis. The glycine substitution was selected because it would allow the greatest exploration of backbone conformations and thus potentially allow a relaxation of steric clashes between backbone and side chain atoms. The alanine substitution retains the restriction of the allowed backbone conformations to those of lysine and other side chains containing a β -carbon, but eliminates any hydrophobic or charge–charge interactions in which the remainder of the Lys 116 side chain might participate.

The effects of these substitutions on the conformational equilibrium of the loop segment were examined through NMR spectroscopy and X-ray crystallography. NMR spectroscopy was employed to determine the effects of these mutations on the isomerization equilibria and the thermal stability of these two variants. The crystal structures of the two variant proteins were refined at high resolution to confirm the dominant peptide bond configuration predicted by the NMR data, and to determine the detailed conformation of the loops.

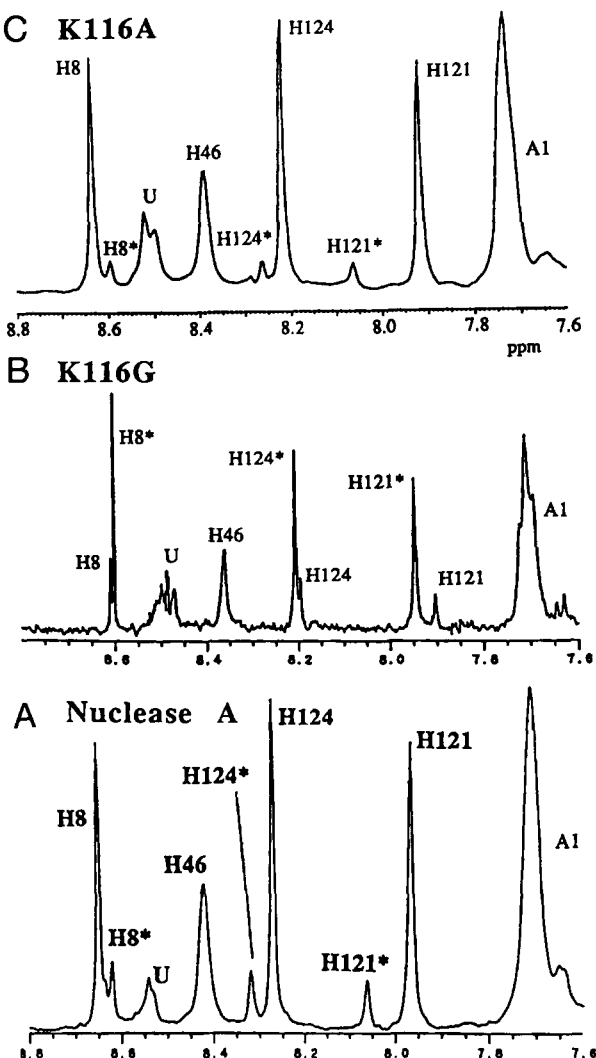


Fig. 1. Low field region of 500-MHz ¹H NMR spectra showing resonances of the four histidine H^{e1} of staphylococcal nuclease A (**A**), the nuclease variant K116G (**B**), and the variant K116A (**C**). The asterisks denote resonances of molecules in which the X 116–Pro 117 peptide bond is *trans*. The backbone amide protons have been exchanged for deuterium, revealing the histidine H^{e1} resonances. Samples are in 200 mM acetic-d₃-acid-d buffered D₂O, pH* 5.3. Spectra A and C were acquired at 40 °C, and are apodized with 2 Hz of line broadening prior to Fourier transformation. Spectrum B was acquired at 45 °C and is resolution enhanced with –0.5 Hz to resolve the multiple resonances of H8 and H124. Spectrum C was recorded on a Bruker AM-500 spectrometer at Yale University; spectra A and B were recorded on a General Electric GN-500 at Stanford.

Results

¹H NMR spectroscopy

The histidine H^{e1} proton region of the NMR spectrum of K116G, shown in Figure 1B, displays major and minor resonances. The presence of multiple resonances for each histidine H^{e1} proton indicates that the K116G substitution has maintained the structural heterogeneity observed in nuclease A. The chemical shifts of the four sets of resonances are sufficiently similar to those of the nuclease A spectrum that the wild-type sequence assignments can

be inferred (Alexandrescu et al., 1988; Kautz et al., 1990), but the relative chemical shifts within each pair of resonances are significantly perturbed so that assignment of the *cis* and *trans* states cannot be made by comparison with nuclease A. For the three resonances where heterogeneity is displayed in nuclease A (H8, H124, H121) the major and minor resonances of K116G appear to be reversed in position when compared to wild-type protein (Fig. 1).

The K116G mutation has either caused a significant alteration in the population of the *cis* and *trans* peptide bond isomers between residues 116 and 117, or it has caused some other structural change which reverses the relative chemical shifts of all three pairs of reporter resonances (H8, H121, H124). The *cis:trans* equilibrium of the Lys 116-Pro 117 peptide bond in nuclease A can be shifted fully to the *cis* conformation by the addition of Ca^{2+} and the competitive inhibitor 3',5'-diphosphothymidine (pdTp). Titration of nuclease A with pdTp in the presence of Ca^{2+} causes a progressive loss of intensity of the *trans* resonances (Evans et al., 1989). We have carried out this experiment with the K116G nuclease variant, as shown in Figure 2. The spectrum of the protein in the absence of ligands is shown in Figure 2A. The addition of Ca^{2+} (Fig. 2B) does not significantly perturb the spectrum. The further addition of pdTp (Fig. 2C-E) increases the intensity of each minor resonance (H8*, H121*, H124*) and diminishes the major resonances (H8*, H121*, H124*). This behavior suggests that the downfield resonance H121* represents the *trans*-Pro 117 conformation, as in the spectrum of nuclease A (see Table 1). Thus, the *trans* Lys 116-Pro 117 conformation is favored in the K116G variant, whereas the *cis* conformation is favored in nuclease A.

The ^1H NMR spectrum of the nuclease K116A mutant is shown in Figure 1C. This spectrum is nearly identical to that of nuclease A (Fig. 1A), suggesting that the *cis* Ala 116-Pro 117 configuration predominates in solution. The H121*, H124*, and H8* resonances are slightly less intense in K116A than in the nuclease A spectrum, indicating that the K116A substitution favors the *cis* peptide bond configuration slightly more than nuclease A does ($\Delta\Delta G = -0.3 \text{ kcal/mol}$; see Table 1).

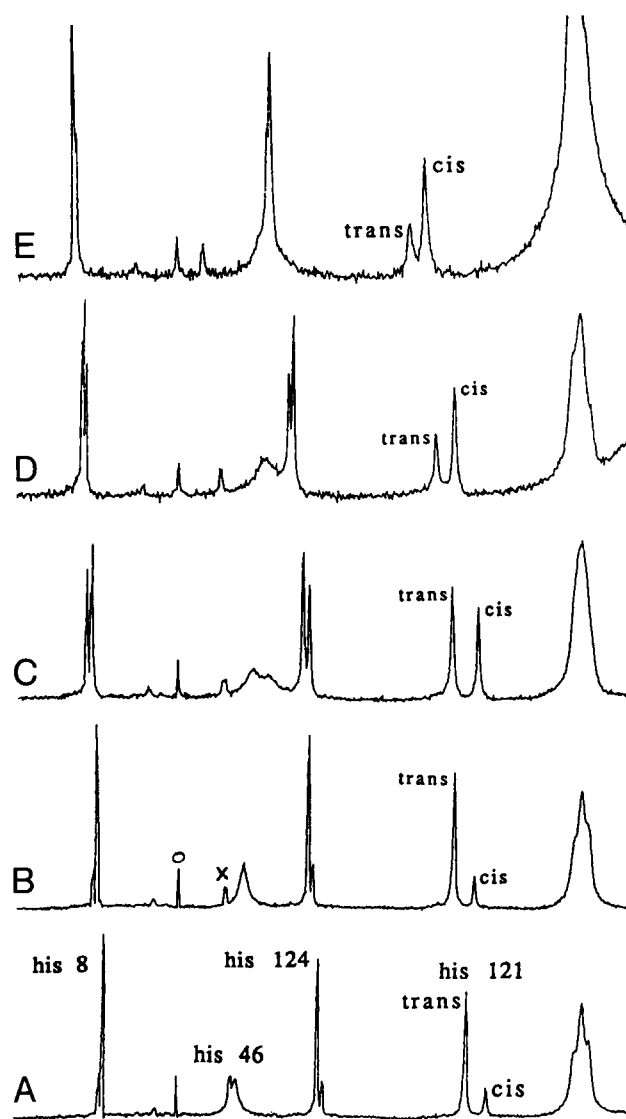


Fig. 2. Effect of ligand binding on the ^1H NMR spectrum of variant K116G. **A:** pH 5.3, 40 °C in 200 mM deuterated acetate-buffered D_2O , no added ligands. **B:** As in A, but with 10 mM CaCl_2 added. **C-E:** As in B, but with addition of 3',5'-diphosphothymidine (pdTp) to 1.0 mM (C), 10 mM (D), and 20 mM (E). Intensity can be seen to shift from the N^* form to the N form as inhibitor is added. The O denotes a formate contaminant in the sample; x is believed to be a minor resonance of His 46 due to *cis:trans* isomerism at the adjacent Pro 47.

Table 1. Thermodynamic measurements^a

	% <i>cis</i> (at 40 °C)	$\Delta G_{\text{cis} \rightarrow \text{trans}}$ (kcal/mol)	T_m (°C)
Nuclease A	88 (1)	1.1 (0.1)	49 (1)
K116A	92 (2)	1.5 (0.2)	50 (1)
K116G	20 (2)	-0.9 (0.2)	54 (1)

^a The uncertainty for each value is expressed in parentheses.

^{13}C NMR spectroscopy

The ratios of major and minor His $\text{H}^{\pm 1}$ proton resonances for the K116G variant indicate an exceptionally wide range in the *cis* peptide bond population as a function of pdTp concentration (20–60%). In light of this phenomenon, K116G was chosen to make a comparison of the ratio of the major and minor histidine ^1H resonances with the *cis:trans* equilibrium of Pro 117 observed directly using [4- ^{13}C]proline-labeled samples. The ^{13}C NMR resonances of the proline C-4 carbon nucleus have been used

to monitor the proline *cis:trans* isomerization state in proteins (Dorman & Bovey, 1973; Sarkar et al., 1984; Stanzyk et al., 1989; Torchia et al., 1989). Figure 3 shows ^{13}C NMR spectra of labeled nuclease A and K116G at several pdTp concentrations. The resonance in Figure 3A labeled P117_{cis} was assigned based on its absence from similar spectra of [4- ^{13}C]Pro-labeled P117G (Stanzyk et al., 1989). The spectrum in Figure 3B shows a resonance labeled P117_{trans} that is not apparent in Figure 3A, and that diminishes in intensity as inhibitor is added while P117_{cis} gains proportionally. The small cluster of ^{13}C resonances at 22.8 ppm may arise from natural abundance non-prolyl residues or from *cis:trans* heterogeneity of other prolines (Wang et al., 1990). In all spectra,

the relative intensities of the *cis* and *trans* Pro 117 resonances in the ^{13}C NMR spectra agree within experimental error with the ratio of major and minor proton resonances of His 121: $19 \pm 3\%$ *cis* (^1H) and $19 \pm 4\%$ *cis* (^{13}C) in the absence of ligands; $41 \pm 3\%$ (^1H) and $40 \pm 4\%$ (^{13}C) at 1 mM pdTp, 10 mM CaCl_2 ; and $62 \pm 3\%$ (^1H) and $63 \pm 4\%$ (^{13}C) at 12 mM pdTp, 10 mM CaCl_2 .

Thermal stability

As outlined in Materials and methods, the T_m of both variant proteins was measured from NMR spectra and the results are shown in Table 1. K116G was found to be more stable to heat denaturation than nuclease A, whereas K116A has a stability comparable to that of nuclease A.

Crystallography

The crystal structures of K116A and K116G are very similar to that of nuclease A except in the region of the mutation and a disordered loop. Each of the two variant structures were superimposed over the nuclease A structure (Hynes & Fox, 1991) by minimizing the differences between the coordinates of the α -carbon positions except those in the loop containing the mutation (residues 111–119) and those of a disordered loop (residues 44–51). The root mean square deviation of backbone atoms of the selected residues from the nuclease A structure is 0.19 Å for K116A and 0.20 Å for K116G (Figs. 4, 7A; Kinemage 1). These changes are of the order of the mean error of atomic positions calculated with a Luzzati plot (Fig. 5) (Luzzati, 1952). The patterns of average isotropic temperature factors per residue for nuclease A and the two variants are also very similar (Fig. 6). Thus, very little change

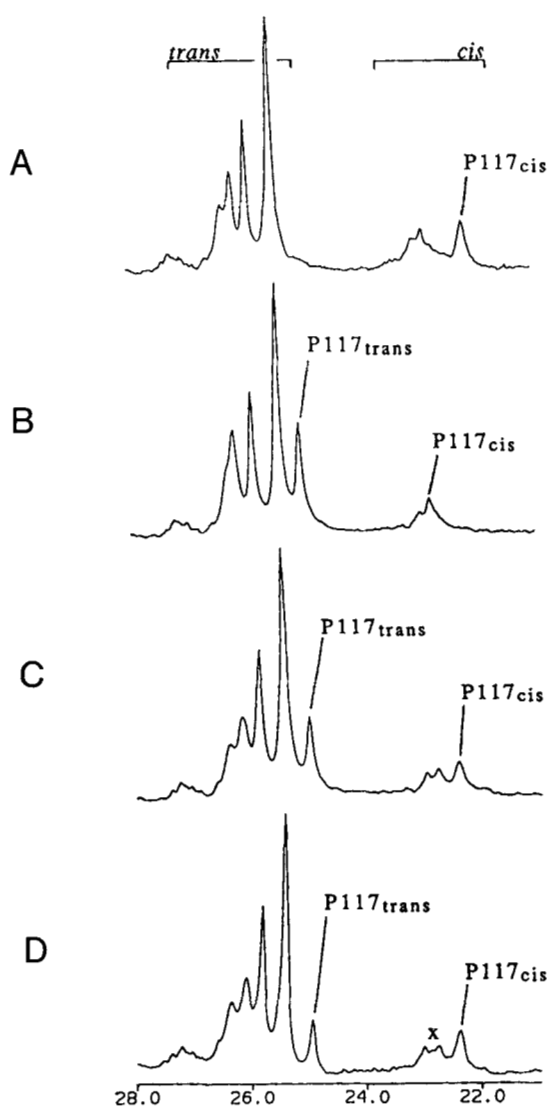


Fig. 3. ^{13}C NMR spectra of nuclease A and the variant K116G in which all six prolines are labeled with ^{13}C at the C-4 position; taken at 40 °C. **A:** Nuclease A. **B:** K116G in the absence of ligands. **C:** As in B, but with the addition of 10 mM CaCl_2 and 1 mM 3',5'-diphosphothymidine (pdTp). **D:** As in C, but with 12 mM pdTp.

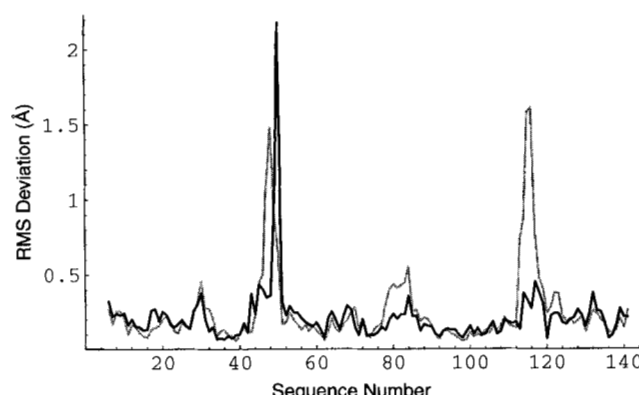


Fig. 4. Plots of the root mean square difference in backbone atom position versus sequence number when comparing K116A (black line) and K116G (gray line) to the structure of nuclease A (Hynes & Fox, 1991). Each of the two variant structures was superimposed over the nuclease A structure by minimizing the differences between the coordinates of the α -carbons of all residues except those in the loop of mutation (residues 111–119) and those of a disordered loop (residues 44–51).

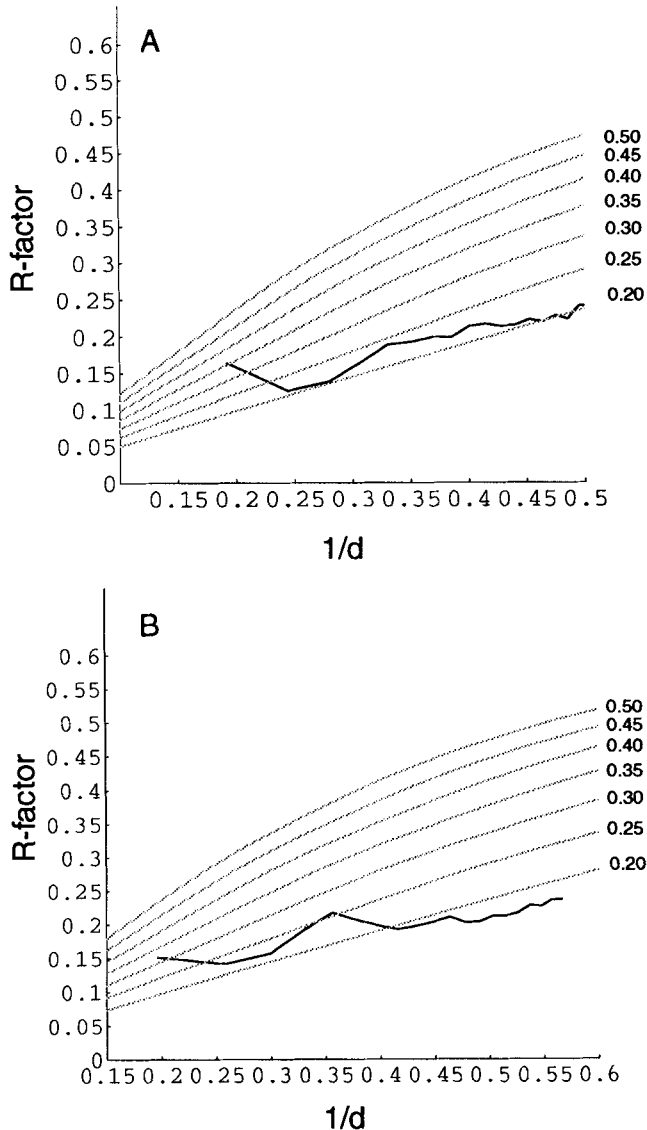


Fig. 5. Luzzati plots (Luzzati, 1952) of the mean atomic error for the K116A (**A**) and the K116G (**B**) structures, where d is the Bragg spacing.

in the global protein structure took place as a result of these substitutions at Lys 116.

The disordered loop of residues 44–51, a region 20 Å away from the mutation site, adopted a different conformation in each variant structure (see Figs. 4, 7A). This loop region is characterized by weak and discontinuous electron density along with elevated temperature factors ($\sim 60 \text{ \AA}^2$; see Fig. 6) in each protein structure indicating that this segment is poorly defined by the experimental data. Although refinement carries the loop of each variant to a different conformation, the details of these conformations are not easily interpretable.

Few changes in the structure of K116A can be seen in the loop containing the mutation when compared to the

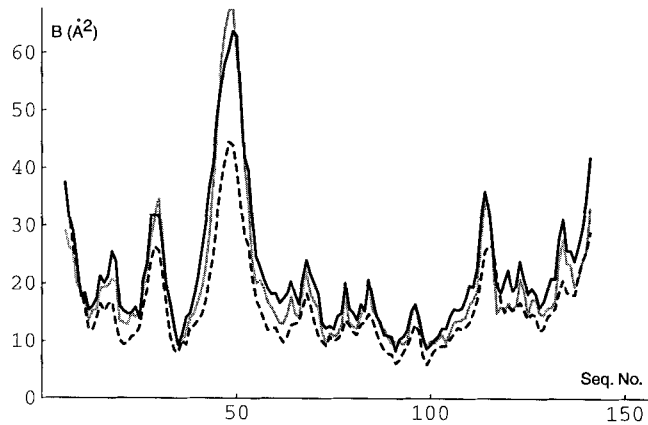


Fig. 6. The average B -factor for the backbone atoms of each residue is plotted for nuclease A (dashed line), K116A with the occupancy of residues 112–117 set to 0.9 (black, unbroken line), and K116G with the occupancy of residues 112–117 set to 0.8 (gray line). The variance in the magnitude of the temperature factors between nuclease A and the two variant structures probably reflects the differences in the final refinement methods. Nuclease A was subjected to Konnert–Hendrickson refinement in its final stages, whereas both variant structures were refined by X-PLOR.

nuclease A structure. Although the loop is conformationally heterogeneous, the density is unambiguous in the first simulated annealing (SA)-omit map (Fig. 8A). This omit map was calculated as described in Materials and methods by omitting residues 112–118 from the model of nuclease A. The SA-omit procedure has proven effective in the reduction of phase bias from electron density maps (Hodel et al., 1992). In this initial map, the conformation of the backbone of residues 112–118 is clearly defined. When superimposed on the nuclease A structure, the imino ring of Pro 117 has rotated slightly such that the γ -carbons of the two models are 0.5 Å apart (Fig. 7B; Kinenage 2). This slight reorientation of the proline ring brings the γ -carbon of the proline in the variant protein 0.2 Å closer to the α -carbon of Gly 79, a residue of a nearby loop. Other than this minor shift, the entire loop structure of K116A is indistinguishable from the nuclease A loop conformation. The similarity can further be demonstrated by comparing the ϕ, ψ dihedral angles of the backbone of the two loops (Fig. 9).

The differences between the K116G variant and the structures of nuclease A and the K116A variant are confined to the disordered loop of residues 44–51, discussed above, and a short solvent-exposed region consisting of residues 112–117. These differences begin with the peptide bond between residues 116 and 117. This bond is *trans* in the K116G structure, where a *cis* configuration was found in the nuclease A and K116A crystal structures. Strong density for the carbonyl oxygen of Gly 116, appearing in a SA-omit map of the proline region (Fig. 8B), clearly defines the *trans* peptide bond. This isomerization

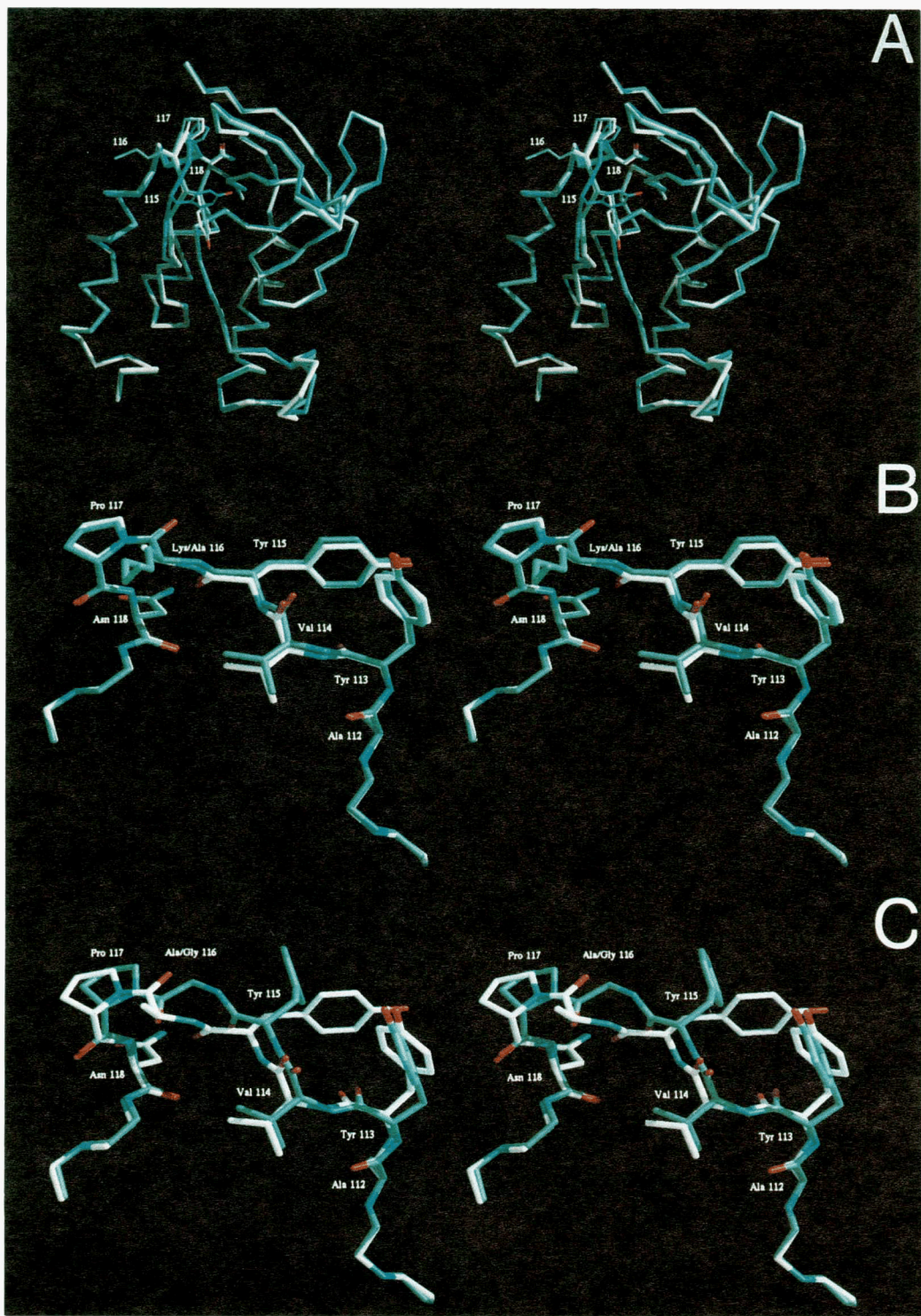


Fig. 7. **A:** Stereo representation of the backbone of nuclease A (white), K116A (green), and K116G (blue). The three structures were superimposed by minimizing the difference between the coordinates of the backbone atoms of all residues except the disordered loop of residues 44–51 and the loop containing the mutation (residues 111–119). The side chains of residues 115–118 are included in the figure. **B:** Stereo representation of the solvent-exposed loop of residues 112–118 from the nuclease A and K116A structures. The structures were superimposed as in A. Carbon atoms from nuclease A are shown in green and K116A carbon atoms are shown in white. **C:** Stereo representation of the solvent-exposed loop of residues 112–118 from the K116A and K116G structures. The structures were superimposed as in A. Carbon atoms from K116G are shown in green and K116A carbon atoms are shown in white. All oxygen atoms are shown in red and all nitrogen atoms are shown in blue.

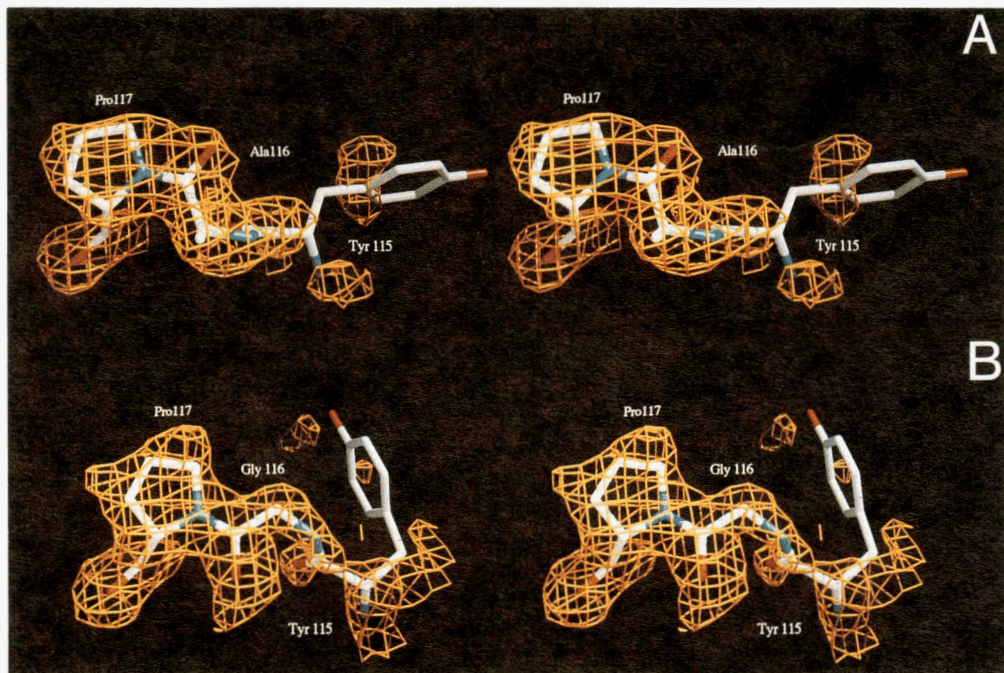


Fig. 8. Stereo representation of the electron density surrounding residues 116 and 117 in the K116A (**A**) and K116G (**B**) structures. Shown are the SA-omit $F_o - F_c$ maps calculated using the nuclease A model (Hynes & Fox, 1991) with residues 112–118 omitted. Each map clearly shows the isomerization state of the 116–117 peptide bond. A detailed description of this calculation is given in the Materials and methods section. Note that this is a map from the earliest point in the refinement. SA-omit maps have reduced phase bias, but they also suffer from weakened density in the area of omission (Hodel et al., 1992). Further refinement of the model produced stronger maps in which the Tyr 115 side chain appears in the position shown. The K116A map is contoured at 1.75σ . The K116G map is contoured at 1.5σ . Carbon atoms are shown in white, oxygen atoms are shown in red, and nitrogen atoms are shown in blue.

leads to large changes in the conformation of the loop in this region. Residues 113–117 appear to bow out from the protein slightly (Fig. 7A,C; Kinemage 2). This may be a result of the increased distance (approx. 0.8 Å) between the 116 and 117 α -carbons imposed by the *trans* isomer in comparison to the *cis* isomer. In the nuclease A and the K116A structures, residues 115–118 are found in a type IVa β -turn. In both structures, a hydrogen bond exists between the backbone carbonyl oxygen of Asn 118 and the backbone amide of Tyr 115, defining the characteristic β -turn geometry. In the K116G structure, residues 115–117 are shifted about 0.5 Å toward the N-terminus of the loop and the Tyr 115–Asn 118 hydrogen bond does not exist (Kinemage 2). As shown in Figure 9, Gly 116 resides in a region of ϕ, ψ space that is forbidden to all other amino acids. If an alanine were to adopt the conformation of Gly 116, the β -carbon would make unfavorable contacts (shown in Kinemage 2) with the δ -carbon of Pro 117 (at a distance of 3.0 Å) and the backbone carbonyl oxygen of Tyr 115 (at a distance of 2.7 Å). Residues 115–118 are no longer in a defined reverse turn conformation. By the criterion offered by Lewis et al. (1973), a reverse turn is defined as a nonhelical segment of residues where $C\alpha_i$ and $C\alpha_{i+3}$ are less than 7 Å apart.

The α -carbons of residues 115 and 118 are 7.39 Å apart in K116G compared to the distance of 5.8 Å found in the nuclease A and K116A models. The significant change in the loop conformation is also apparent from a comparison of the backbone dihedral angles of this loop to those of K116A and nuclease A (Fig. 9).

There are few contacts between the six residue loop (residues 112–117) containing the mutation and its protein context. The primary restraint imposed on the conformation of the loop by the protein is the anchorage of the loop at residues 111 and 118. Val 111 is buried within the protein surface making multiple intramolecular packing contacts (Kinemage 3). Asn 118 is rigidly fixed in its place by hydrogen bonds between its side chain and nearby residues of the protein structure (Kinemage 4). The amide nitrogen hydrogen bonds to the backbone carbonyl oxygen of residue 80, and the δ -oxygen of 118 bonds to the backbone nitrogen of residue 79. Because of these interactions, Val 111 and Asn 118 are found in an identical conformation in the nuclease A, K116A, and K116G crystal structures. The only other contacts made between this loop and the protein occur as intramolecular contacts with Pro 117, which contacts Gly 79 from a nearby loop, and Val 114, whose side chain is oriented toward the pro-

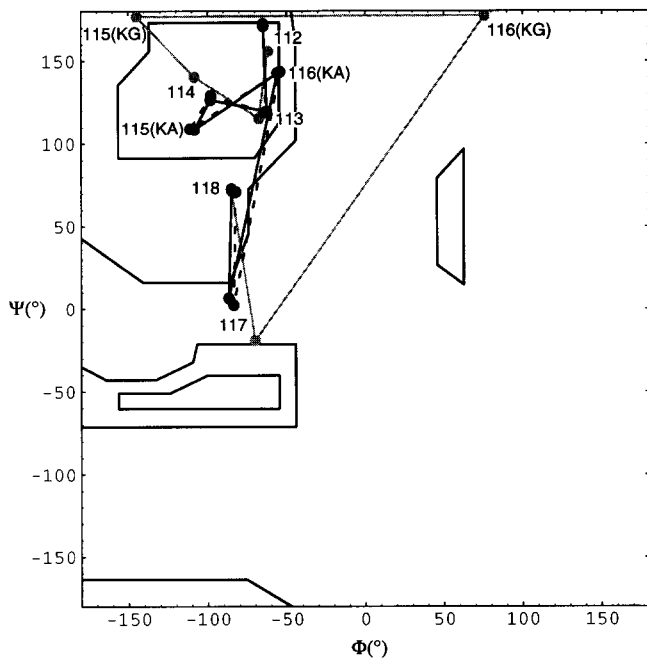


Fig. 9. The backbone dihedral angles of residues 112–118 for nuclease A (dashed line), K116A (black, unbroken line), and K116G (gray line) are shown. The ϕ - ψ angles of each residue are denoted by dots connected by lines. Each ϕ - ψ pair is labeled with the number of the corresponding residue. Residues with distinct conformations for K116A and K116G are labeled KA and KG, respectively.

tein and packs loosely with the side chains of Leu 38 and Glu 122. These contacts are also present in all three crystal structures.

Discussion

Two mutations were characterized to identify the role of Lys 116 in establishing the *cis:trans* equilibrium of the Lys 116-Pro 117 peptide bond in staphylococcal nuclease A. Nuclease A favors a *cis* peptide bond between Lys 116 and Pro 117 (88%). Replacement of Lys 116 with Gly results in a predominantly *trans* (~80%) configuration at the 116–117 peptide bond, whereas the *cis* configuration is favored when Ca^{2+} and a 3',5'-diphosphonucleotide competitive inhibitor are bound. [4- ^{13}C]-Proline-labeled protein has been used to confirm the *cis:trans* ratio at Pro 117 derived from the histidine $\text{H}^{\epsilon 1}$ resonances. An Ala 116 substitution results in a predominantly *cis* 116–117 peptide bond configuration similar to that observed in nuclease A. The 116–117 peptide bond is *trans* in the K116G X-ray structure and *cis* in the K116A structure. The quantitative correlation between the ^1H and ^{13}C NMR measurements, and the agreement between the dominant isomerization state predicted by NMR and observed in the X-ray structures provides further strong support that the heterogeneity observed in the histidine $\text{H}^{\epsilon 1}$ resonances monitors *cis:trans* isomerization at Pro 117.

The differences between the structures of nuclease A, K116A, and K116G are confined to two loop regions: a disordered loop at residues 44–51 and the loop of mutation at residues 112–117. The loop at residues 44–51 is poorly defined, but the discontinuous electron density in this region suggests that each variant adopts a different conformation in this segment. The conformational variation in this loop may be due to long range effects of the mutation or to the reaction of a flexible loop to different solution conditions (such as precipitant concentration). The lack of information in this region prohibits a detailed interpretation.

Other than this disordered region, nuclease A, K116A, and K116G all have identical protein structures except for the conformation of residues 112–117, which changes dramatically in K116G (Kinemage 2). Localized changes in the loop conformation with amino acid substitution were also observed in previous variants where Pro 117 was mutated to a glycine and a threonine (Hynes & Fox, in prep.). Although nuclease is able to accommodate a variety of conformations in this loop without altering the rest of its structure, these residues adopt ordered conformations that are well defined in each of the crystal structures. Thus a combination of the backbone and side chain interactions within the loop sequence, the position and orientation of the loop anchorage, and the interactions with the solvent provides sufficient restraints such that a dominant loop conformation is populated. The two variants examined here provide examples of this situation for loops with both *cis* and *trans* peptide bonds. This suggests that the minor folded forms of these two variants may also adopt single, well-defined conformations.

A comparison of these variant structures suggests that, in the context of this β -turn, the only interactions that affect the conformation of these residues are those involving the backbone atoms and the β -carbons. Under this hypothesis, all amino acids are equivalent to alanine except proline and glycine. In the proteins presented here, the mutation of a fully solvated Lys 116 residue to an alanine resulted in an almost identical protein structure. The NMR studies show that K116A and nuclease A possess very similar thermodynamic properties as well. Thus, experimentally, Ala 116 is equivalent to lysine. The mutation of Lys 116 to a glycine resulted in a protein in which residue 116 adopts a conformation forbidden to all non-glycine amino acids. Because this change appears with the removal of the β -carbon methyl group of Ala 116, and because the glycine is in this forbidden region of ϕ , ψ space for alanine, the interactions responsible for the change in the conformation of the loop when comparing K116A and K116G are most certainly local backbone interactions with the β -carbon.

The equilibrium between the *cis* and *trans* forms of nuclease therefore appears to be determined by the interplay between local backbone interactions, dictated by the primary sequence of the loop, and the position of the loop

ends anchored by residues 111 and 118. Nuclease A and K116A adopt a *cis* peptide bond between residues 116 and 117, whereas in short peptides (Grathwohl & Wüthrich, 1976), in peptide analogues of this sequence (Raleigh et al., 1992), and in the unfolded nuclease (Evans et al., 1989) the *trans* X-Pro peptide bond is favored. One explanation for this phenomenon is that the position of the ends of the loop only allow *trans* conformations where the local backbone interactions associated with the ϕ and ψ torsion angles are strained. When the 116–117 peptide bond is *cis*, less strained backbone conformations are available. Thus the relaxation of the backbone strain intrinsic to the *trans* conformation compensates for the energetically unfavorable *cis* X-Pro peptide bond. With the removal of the side chain from residue 116 (K116G), the backbone strain of the *trans* conformation is reduced to the point that the conformation associated with the *cis* peptide bond is no longer favorable. Thus the change in the equilibrium between these two variants can be described as the choice between backbone strain associated with unfavorable ϕ , ψ torsion angles versus the higher energy of the *cis* peptide bond. If the *trans* conformation of K116A is similar to that observed in the K116G crystal structure, then this "backbone strain" most probably involves the steric clash between the β -carbon of Ala 116 and either the carbonyl oxygen of Tyr 115, the δ -carbon of Pro 117, or both.

Other mutations outside of the loop sequence that stabilize the *trans* configuration relative to the *cis* configuration have been reported by Alexandrescu et al. (1990). In these mutants, $\Delta G_{cis \rightarrow trans}$ was inversely correlated with $\Delta G_{unfolding}$. This correlation is not observed in our variants where K116G is more stable than nuclease A. If protein stress induces a strained conformation in the loop through the anchorage of the loop ends, there are two ways to relieve that strain. First, the rigidity of the loop anchorage could be reduced by destabilizing the protein, allowing less strained conformations to be populated. This can be achieved by changing the solvent conditions such as pH and temperature (Alexandrescu et al., 1989) or by destabilizing mutations in the protein outside of the loop (Alexandrescu et al., 1990). In such mutations, one would expect $\Delta G_{cis \rightarrow trans}$ to be inversely correlated with $\Delta G_{unfolding}$, as is the case.

A second way to affect the 116–117 *cis:trans* equilibrium is to reduce the backbone strain within the loop by removing steric clashes between side chain and backbone atoms and allowing greater exploration of ϕ , ψ space. $\Delta G_{unfolding}$ should be correlated rather than inversely correlated with $\Delta G_{cis \rightarrow trans}$ for such mutants, as the removal of strained interactions should stabilize the protein as a whole. K116G is consistent with this proposal as it allows greater exploration of conformation space, it has a higher fraction of *trans* isomers, and it is more stable to heat denaturation than nuclease A.

A situation where a large change in local conformation accompanies a simple amino acid substitution, as in the case described here, provides a favorable and interesting system for exploration by computer simulation. Computational studies on this system have commenced toward two related goals. First, we wish to predict the major conformations of a loop given the primary sequence and protein context. This sort of prediction could be used to approximate the conformation of the minor folded form of each nuclease variant. The second goal is to determine which of the various intramolecular interactions are important in determining the conformational equilibrium of the loop. The interactions that define the equilibrium between the *cis* and *trans* conformations of nuclease can be explored through free energy simulations.

Materials and methods

Construction of mutant proteins

The point mutants K116A and K116G of staphylococcal nuclease A, the wild-type nuclease from the *Staphylococcus aureus* Foggi strain, were generated by oligonucleotide directed mutagenesis (Zoller & Smith, 1983). The mutagenic oligonucleotides were annealed to single stranded M13 template DNA containing the cloned wild-type nuclease gene. These oligonucleotides were extended using the Klenow fragment, then the extension reaction was transformed into competent cells of the *Escherichia coli* strain JM101. Plaques were transferred to nitrocellulose and probed with 32 P-end-labeled mutagenic oligonucleotides and washed at several temperatures. Positive plaques were sequenced to verify the mutations. They were then subcloned into the pAS1 expression vector and transformed into the *E. coli* strain AR120. The variant protein was expressed and purified as described (Evans et al., 1989). The K116G variant protein was additionally purified through the use of an affinity column composed of the tightly binding nucleotide inhibitor, amino-pdT_p, covalently attached to sepharose. The purified K116G was applied to the affinity column in 50 mM Tris, 20 mM Ca²⁺, pH 8, washed with the same, and eluted with 0.1 M acetic acid, 5 M urea. Each eluted fraction was neutralized with 1 M Tris, pH 8.2, then pooled and dialyzed for 8 h against 1 M NaCl, 200 mM NaCl, and twice more against distilled water. The protein solution was then lyophilized and stored at –20 °C.

¹H NMR

Lyophilized protein (10–30 mg) was suspended in D₂O (99%; Aldrich) and adjusted to pH* 5.3. (pH* refers to glass electrode meter reading uncorrected for deuterium isotope effects [Bundi & Wüthrich, 1979].) The sample was then heated to 10 °C above the T_m for 5 min to fa-

cilitate exchange of labile protons, and any precipitate was removed by centrifugation. The deuterated protein was lyophilized again, and resuspended in 0.5 mL of 200 mM acetic-d₃-acid-d, pH* 5.3, with 1 mM TSP (trimethylsilyl propionate; Aldrich) as a chemical shift reference. Trace precipitate, if present, was removed by centrifugation before transferring to a 5-mm NMR tube.

The fraction *cis* was obtained from the relative areas of the resolved *cis* and *trans* histidine resonances of spectra acquired at 40 °C. The nonlinear least-squares curve fitting of the Lorentzian lines was performed using an adaptation (R.A.K.) of published code for the Leverberg-Marquardt algorithm (Press et al., 1986), run as a user module in Dennis Hare's FTNMR program (version 5.1). The uncertainty is the standard deviation determined by this program. The ΔG values for the *cis:trans* equilibrium were obtained using $\Delta G = -RT\ln(K)$, where K is the equilibrium constant for the isomerization from *cis* to *trans*.

¹³C NMR

Nuclease A and the nuclease mutant K116G were each labeled with [4-¹³C]proline. *E. coli* AR120 cells containing the pAS1 plasmid encoding either nuclease A or K116G were grown in 1 L of M9 minimal medium supplemented with glucose (16 g), biotin (1.6 mg), thiamine (8 mg), niacin (40 mg), and each amino acid (0.22 g) except proline. The cultures were induced at mid-log phase with nalidixic acid (0.08 g). Twenty minutes before induction, 50 mg [4-¹³C]proline was added to the media. Cells batches were processed as described previously (Evans et al., 1989) and yielded 14 mg of nuclease A and 28 mg of mutant protein. One-dimensional ¹³C spectra were collected on a Bruker AM-500 spectrometer at 25 and 40 °C. ¹³C chemical shifts are reported relative to an external standard of dioxane (67.4 ppm). The areas of the Pro 117 *cis* and *trans* ¹³C resonances were measured by performing a nonlinear least-squares fit of Lorentzian lines to the spectrum, as described above. The same method was used to measure the intensities of the resolvable *cis* and *trans* resonances of a histidine proton spectrum acquired after each ¹³C spectrum.

T_m determination

NMR spectra of nuclease, or its variants, in 200 mM acetic-d₃-acid-d buffered D₂O, pH* 5.3, were prepared as described above. The T_m was first estimated from a series of spectra with 5 or 10 °C temperature increments. The T_m was then accurately determined from a series of at least 10 spectra with 2 °C temperature increments, long temperature equilibration, and adjustment of shims before each acquisition. Probe temperatures for each spectrum were read directly from the console variable temperature

control unit. The temperature control unit was calibrated for each experiment using an external digital thermometer with the thermocouple lowered into the probe in an NMR tube with buffer. The relative precision of temperatures in a series was ± 0.1 °C; the absolute accuracy of the temperatures of any series is within 0.5 °C.

Areas of histidine resonances of unfolded protein were measured from spectra by curve fitting. The equilibrium constant of folding (K) was determined for each temperature through nonlinear least-squares fitting as described above. These values were plotted with uncertainties on a van't Hoff plot, $\ln(K)$ vs. $1/T$. The T_m and its uncertainty were determined from the $\ln(K) = 0$ intercepts of the best fit and worst acceptable fit lines.

Crystallography

Both nuclease K116A and K116G variants were crystallized from a low salt buffer (10.5 mM potassium phosphate, pH 8.15) using the precipitant 2-methyl-2,4-pentanediol (MPD), and yielded crystals in space group P4₁, nearly isomorphous with the nuclease A crystals (Arnone et al., 1969). Diffraction data were collected from single crystals of each variant at 5.0 °C using a Xuong-Hamlin two-area detector system (Hamlin, 1985). CuK α X-rays (1.54 Å) were generated by a Rigaku RU-300 rotating anode operating at 40 kV/250 mA. Data reduction and scaling were performed using the data reduction program written by Anderson and Neilsen (Anderson, 1986). Data were only considered up to the D2 value defined as the highest resolution shell with an average intensity greater than 2σ . We collected 58,392 measurements of 11,360 reflections from the K116A crystal ($a = b = 47.84$ Å, $c = 63.34$ Å) covering 95% of the possible reflections to the D2 value of 1.9 Å. The merging R -factor for symmetry-related reflections was 6.3%. The K116G crystal ($a = b = 47.42$ Å, $c = 63.36$ Å) yielded 73,012 measurements of 14,351 unique reflections covering 96% of all possible reflections to the D2 value of 1.75 Å. The merging R -factor for symmetry-related reflections was 7.0% (see Table 2).

The starting phases and coordinates for both structures were derived from the structure of nuclease A (Hynes & Fox, 1991) with the solvent molecules removed. To avoid model bias, residues 112–118, a solvent exposed loop, were omitted from the nuclease A structure. This edited structure was then rigid-body refined to the low resolution diffraction data (15–3 Å), where the entire protein is treated as a rigid body. An overall temperature factor was then computed and applied to the model. Further rigid-body minimization and overall B -factor refinement were performed using data from 15 to 2 Å resolution. With residues 112–118 still omitted, the model was refined to the original data using alternate cycles of positional and individual restrained B -factor refinement to final R -values of 25.1% for K116A and 24.8% for K116G. All re-

Table 2. Crystallographic and geometric parameters at the end of refinement

	K116A	K116G
<i>a, b</i>	47.84	47.42
<i>c</i>	63.34	63.36
Resolution range (Å)	6.0–1.9	6.0–1.75
Number of reflections	10,420	12,342
<i>R</i> _{symmetry} ^a	6.3%	7.0%
<i>R</i> -factor ^b	18.7	18.8
Number of protein atoms	1,088	1,087
Number of water atoms	63	60
Number of total atoms	1,151	1,147
Mean <i>B</i> -factor	26.0	23.4
Main chain atoms	21.9	19.7
Side chain atoms	28.2	26.2
Water	43.0	31.1
Deviations from ideal geometry		
Bond lengths (Å)	0.014	0.013
Bond angles	2.8°	2.7°
Dihedral angles	24.1°	23.5°
Improper angles (planar and chirality)	1.7°	1.7°

^a Merging *R*-factor for symmetry-related reflections, defined as $\Sigma|F_c - I|/\Sigma|I\rangle$.

^b Crystallographic *R*-factor, defined as $\Sigma|F_o - F_c|/\Sigma F_o$.

finement, including rigid-body minimization, positional, *B*-factor, and simulated annealing refinements were carried out through the program X-PLOR (Brünger et al., 1987).

Nuclease crystals diffract anisotropically, with stronger amplitudes along the *c** axis relative to the *a** and *b** axes. To correct this anisotropy, the original data was scaled to the calculated data using a local scaling program (Hynes & Fox, 1991) adapting the methods of Matthews and Czerwinski (1975). In this procedure, a local scale factor is calculated as $\Sigma(F_c)/\Sigma(F_o)$ for a $5 \times 5 \times 5$ (hkl units) box of reflections excluding the central reflection to prevent bias. The resulting scale factor is applied to the central F_o , which was omitted. Prior *B*-factor refinement of the model to the original data should preserve the overall temperature factor information in the anisotropic scaling of the data.

The model of each variant was then refined using the simulated annealing omit procedure (Hodel et al., 1992) using data from 6 to 1.9 Å resolution. This is a procedure whereby the homologous part of the structure may be refined by simulated annealing minimizing phase bias in the unknown region of the model. Residues 112–118 were omitted from the structure, and the residues within 3 Å of this loop were harmonically restrained to their current positions. This edited and restrained structure was annealed from a starting temperature of 4,000 K using the slow cool protocol (Brünger et al., 1990). The *R*-factor of the new model with the loop omitted was 24.2% for

K116A and 23.3% for K116G. The $F_o - F_c$ omit map from these partial structures were studied using the program FRODO (Jones, 1985) on an Evans and Sutherland PS390 workstation. The maps contained clear density along the backbone trace of residues 112–118 when contoured at 1.25σ. The side chains of Tyr 113 and Tyr 115 were not clearly represented in the SA-omit maps in either variant, and were therefore removed from the models in the initial refinement procedures.

The K116A $F_o - F_c$ SA-omit map, again with residues 112–118 omitted from the map calculation, demonstrated a good fit to the nuclease A conformation in the mutated loop region of residues 112–118 when superimposed over the nuclease A structure (Fig. 8A). Thus, without any rebuilding, the lysine of the model was replaced by an alanine to create the first complete model of the structure. This model was then subjected to simulated annealing using a slow-cool protocol (Brünger et al., 1990). The starting temperature for the molecular dynamics was 3,000 K. During the annealing, this temperature was reduced by 25 K every 0.02 ps until 300 K was reached. This produced a structure with an *R*-factor of 22.8%. Further refinement by cycles of positional and *B*-factor refinement brought the *R*-factor to 21.5%. At this point, weak density for the side chains of Tyr 113 and Tyr 115 appeared in $F_o - F_c$ maps contoured at 0.75σ. The tyrosines were added to the model, and their positions and *B*-factors were refined. Restrained *B*-factor refinement of the tyrosine side chains increased the *B*-factors of the backbone to a level which was inconsistent with the quality of the electron density (~40 Å²). This is probably a result of lower occupancy of the modeled side chains due to the existence of multiple rotamer positions of the tyrosines not visible in the map. This situation was resolved by removing the restraints between the tyrosine side chains and the backbone, and then repeating the refinement. This produced reasonable tyrosine *B*-factors (~30 Å² backbone, ~40 Å² side chains) and an *R*-factor of 21.5%. 63 water molecules were added to the model and refined by positional and *B*-factor refinement to a final *R*-factor of 18.7% (see Table 2).

The K116G $F_o - F_c$ SA-omit map showed a loop conformation in weak electron density that was quite different than the conformation of the nuclease A structure including a *trans* 116–117 peptide bond (Fig. 8B). Using FRODO, a model for the backbone of residues 112–118 was built into the density. Then, the complete protein model was annealed using the slow-cool protocol from 3,000 K resulting in an *R*-factor of 23.1%. Next, the model structures from the last two simulated annealing runs, one from the annealing omit and one from the full protein refinement, were compared residue by residue to the maps calculated from each model. This was done in order to visually choose the best side chain conformation for each residue which differed from one model to the next. Simulated annealing can either find a better alter-

Table 3. Multiple refinements with varying loop occupancy

Occupancy of residues 112-117	K116A		K116G	
	Average backbone <i>B</i> -factor of residues 112-117 (\AA^2)	<i>R</i> -factor	Average backbone <i>B</i> -factor of residues 112-117 (\AA^2)	<i>R</i> -factor
	1.0	30.5	18.7	30.8
0.9	27.2	18.7	28.7	18.8
0.8	24.8	18.7	26.2	18.8
0.7	22.4	18.7	23.0	18.9

native conformation or move a side chain away from a correct conformation with weak electron density. This procedure was added to evaluate which of these phenomena occurred for each residue. The resulting model was then refined by alternating positional and *B*-factor refinement to an *R*-factor of 21.8%. The side chains of Tyr 113 and Tyr 115 were added to the model in the same manner used for K116A to yield an *R*-factor of 21.8%. Sixty water molecules were added and the model was then refined to a final *R*-factor of 18.9%.

The solution studies of these proteins suggested that the conformations which were observed in the 112–117 loop region of the protein are present at fractional occupancy. NMR measurements indicate that the major conformation of K116A is present at only 90% occupancy, and that of K116G is present at 80% occupancy. Since occupancy and temperature factors are strongly correlated, it is difficult to determine the occupancy of the six residue loop from the crystallographic data. To determine the effects of changing occupancy on the temperature factors of the loop, the final stages of refinement were performed on four separate models where the occupancy of residues 112–117 was set to 1.0, 0.9, 0.8, and 0.7. The results of these refinements are shown in Table 3. The *R*-factor for each of these refinements is identical showing the difficulty of discriminating between the different occupancies. As expected, the *B*-factors decrease with decreasing occupancy. For consistency with the solution studies, we have reported the temperature factors from the 0.9 occupancy model of K116A and the 0.8 occupancy model of K116G. No alternative conformation could be fit to the residual difference maps of this loop region.

The coordinates of both K116A and K116G have been submitted for deposit with the Brookhaven Protein Data Bank.

Acknowledgments

This work was supported by NIH grants to R.O.F. (AI23923), by the Howard Hughes Medical Institute, and by shared instrumentation grants to Stanford University and Yale University

(NIH RR03475, NSF DMB8610557, and ACS RD259) for the NMR spectrometers. A.H. is a Howard Hughes Medical Institute Predoctoral Fellow. M.D.J. is an NSF predoctoral fellow. We acknowledge the assistance of Richard Austin in preparing the ^{13}C -labeled samples. [4- ^{13}C]Proline was a generous gift from Dr. Dennis Torchia. We thank Drs. A.T. Brünger, C.M. Dobson, P.A. Evans, R.L. Baldwin, and F.M. Richards for helpful discussions.

References

- Alexandrescu, A.T., Hinck, A.P., & Markley, J.L. (1990). Coupling between local structure and global stability of a protein: Mutants of staphylococcal nuclease. *Biochemistry* 29, 4516–4525.
- Alexandrescu, A.T., Mills, D.A., Ulrich, E.L., Chinami, M., & Markley, J.L. (1988). NMR assignments of the four histidines of staphylococcal nuclease in native and denatured states. *Biochemistry* 27, 2158–2165.
- Alexandrescu, A.T., Ulrich, E.L., & Markley, J.L. (1989). Hydrogen-1 NMR evidence for three interconverting forms of staphylococcal nuclease: Effects of mutations and solution conditions on their distribution. *Biochemistry* 28, 204–211.
- Anderson, D.H. (1986). The use of a multiwire area detector diffractometer, the crystal structure of the compound I decay product of cytochrome *c* peroxidase, and a crystallographic study of phospholipase A2. Ph.D. Thesis, University of San Diego, San Diego.
- Arnone, A., Bier, C.J., Cotton, F.A., Hazen, E.E., Jr., Richardson, D.C., & Richardson, J.S. (1969). The extracellular nuclease of *Staphylococcus aureus*: Structure of the native enzyme and an enzyme-inhibitor complex at 4 \AA resolution. *Proc. Natl. Acad. Sci. USA* 64, 420–427.
- Brünger, A.T., Kruckowski, A., & Erickson, J.W. (1990). Slow cooling protocols for crystallographic refinement by simulated annealing. *Acta Crystallogr. A* 46, 585–593.
- Brünger, A.T., Kurian, J., & Karplus, M. (1987). Crystallographic *R* factor refinement by molecular dynamics. *Science* 235, 458–460.
- Bundi, A. & Wüthrich, K. (1979). ^1H -NMR parameters of the common amino acid residues measured in aqueous solutions of the linear tetrapeptides H-gly-gly-X-ala-OH. *Biopolymers* 18, 285–297.
- Calderon, R.O., Stolowich, N.J., Gerlt, J.A., & Sturtevant, J.M. (1985). Thermal denaturation of staphylococcal nuclease. *Biochemistry* 24, 6044–6049.
- Cotton, F.A., Hazen, E.E., Jr., & Legg, M.J. (1979). Staphylococcal nuclease: Proposed mechanism of action based on structure of enzyme-thymidine 3',5'-bisphosphate-calcium ion complex at 1.5 \AA resolution. *Proc. Natl. Acad. Sci. USA* 76, 2551–2555.
- Dorman, D.E. & Bovey, F.A. (1973). ^{13}C magnetic resonance spectroscopy of proline in oligopeptides. *J. Org. Chem.* 38, 2379–2383.
- Evans, P.A., Dobson, C.M., Kautz, R.A., Hatfull, G., & Fox, R.O. (1987). Proline isomerism in staphylococcal nuclease characterized by NMR and site-directed mutagenesis. *Nature* 329, 2266–2268.
- Evans, P.A., Kautz, R.A., Fox, R.O., & Dobson, C.M. (1989). A magnetization-transfer nuclear magnetic resonance study of the folding of staphylococcal nuclease. *Biochemistry* 28, 362–370.
- Fox, R.O., Evans, P.A., & Dobson, C.M. (1986). Multiple conformations of a protein demonstrated by magnetization transfer NMR spectroscopy. *Nature* 320, 192–194.
- Grathwohl, C. & Wüthrich, K. (1976). The X-Pro peptide bond as an NMR probe for conformational studies of flexible linear peptides. *Biopolymers* 15, 2025–2041.
- Hamlin, R. (1985). Multiwire area X-ray diffractometer. *Methods Enzymol.* 114, 416–452.
- Herzberg, O. & Moult, J. (1991). Analysis of the steric strain in the polypeptide backbone of protein molecules. *Proteins Struct. Funct. Genet.* 11, 223–229.
- Hodel, A., Kim, S.-H., & Brünger, A.T. (1992). Model bias in macromolecular crystal structures. *Acta Crystallogr. A* 48, 851–858.
- Hynes, T.R. & Fox, R.O. (1991). The crystal structure of staphylococcal nuclease refined at 1.7 \AA resolution. *Proteins Struct. Funct. Genet.* 10, 92–105.
- Kautz, R.A. & Fox, R.O. (1991). Multiple conformations of staphylo-

- coccal nuclease. In *Techniques in Protein Chemistry II* (Villafranca, J.J., Ed.), pp. 263–274. Academic Press, San Diego, California.
- Kautz, R.A., Gill, J.A., & Fox, R.O. (1990). Assignment of histidine resonances in the NMR spectrum of staphylococcal nuclease using site-directed mutagenesis. In *Protein and Pharmaceutical Engineering* (Craik, C., Ed.), pp. 1–15. Wiley-Liss, New York.
- Kuwajima, K., Okayama, N., Yamamoto, K., Ishihara, T., & Sugai, S. (1991). The Pro 117 to glycine mutation of staphylococcal nuclease simplifies the unfolding-folding kinetics. *FEBS Lett.* **290**, 135–138.
- Jones, T.A. (1985). Interactive computer graphics: FRODO. *Methods Enzymol.* **115**, 252–270.
- Lewis, P.N., Momany, F.A., & Scheraga, H.A. (1973). Chain reversals in proteins. *Biochim. Biophys. Acta* **303**, 211–229.
- Loll, P.A. & Lattman, E.E. (1989). The crystal structure of the ternary complex of staphylococcal nuclease, Ca^{2+} , and the inhibitor pdTp, refined at 1.65 Å. *Proteins Struct. Funct. Genet.* **5**, 183–201.
- Luzzati, V. (1952). Traitement statistique des erreurs dans la détermination des structures cristallines. *Acta Crystallogr.* **5**, 802–810.
- Markley, J.L., Williams, M.N., & Jardetzky, O. (1970). Nuclear magnetic resonance studies of the structure and binding sites of enzymes, XII. A conformational equilibrium in staphylococcal nuclease involving a histidine residue. *Proc. Natl. Acad. Sci. USA* **65**, 645–651.
- Matthews, B.W. & Czerwinski, E.W. (1975). Local scaling: A method to reduce systematic errors in isomorphous replacement and anomalous scattering measurements. *Acta Crystallogr. A* **31**, 480–487.
- Press, W.H., Flannery, B.P., Teukolsky, S.A., & Vetterling, W.T. (1986). *Numerical Recipes*. Cambridge University Press, Cambridge, UK.
- Raleigh, D.P., Evans, P.A., Pitkeathly, M., & Dobson, C.M. (1992). A peptide model for proline isomerism in the unfolded state of staphylococcal nuclease. *J. Mol. Biol.* **228**, 338–342.
- Sarkar, S.K., Young, P.E., Sullivan, C.E., & Torchia, D.A. (1984). Detection of *cis* and *trans* X-Pro peptide bonds in proteins by ^{13}C NMR – Application to collagen. *Proc. Natl. Acad. Sci. USA* **81**, 4800–4803.
- Serpersu, E.H., Shortle, D., & Mildvan, A.S. (1986). Kinetic and magnetic resonance studies of effects of genetic substitution of a Ca^{2+} liganding amino acid in staphylococcal nuclease. *Biochemistry* **25**, 68–77.
- Shortle, D.J. & Meeker, A.K. (1986). Mutant forms of staphylococcal nuclease with altered patterns of guanidine hydrochloride and urea denaturation. *Proteins Struct. Funct. Genet.* **1**, 81–89.
- Stanzyk, S.M., Bolton, P.H., Dell'Acqua, M., & Gerlt, J.A. (1989). Observation and sequence assignment of a *cis* prolyl peptide bond in unliganded staphylococcal nuclease. *J. Am. Chem. Soc.* **111**, 8317–8318.
- Torchia, D.A., Sparks, S.W., & Bax, A. (1989). Proline assignments and identification of the *cis* K116/P117 peptide bond in liganded staphylococcal nuclease using isotope edited 2D NMR spectroscopy. *J. Am. Chem. Soc.* **28**, 5509–5524.
- Tucker, P.W., Hazen, E.E., & Cotton, F.A. (1979). Staphylococcal nuclease reviewed: A prototypic study in contemporary enzymology. IV. Nuclease as a model for protein folding. *Mol. Cell. Biochem.* **23**, 131–141.
- Wang, J., Hinck, A.P., Loh, S.N., & Markley, J.L. (1990). Two-dimensional NMR studies of staphylococcal nuclease: Evidence for conformational heterogeneity from hydrogen-1, carbon-13, and nitrogen-15 spin system assignments of the aromatic amino acids in the nuclease H124L-thymidine 3',5'-bisphosphate- Ca^{2+} ternary complex. *Biochemistry* **29**, 4242–4253.
- Zoller, M.L. & Smith, M. (1983). Oligonucleotide-directed mutagenesis of DNA fragments cloned into M13 vectors. *Methods Enzymol.* **100**, 468–500.